

NUMERICAL INVESTIGATION OF FLOW MALDISTRIBUTION IN INLET HEADER OF PRINTED CIRCUIT HEAT EXCHANGER

Yuwen Hua^{1,3}, Yushuang Chen^{1,2*}, Xiaohong Yang¹

¹ Shanghai Institute of Applied Physics, Chinese Academy of Sciences, Shanghai 201800, China

² CAS Innovative Academy in TMSR Energy System, Chinese Academy of Sciences, Shanghai 201800, China

³ ShanghaiTech University, Shanghai 200120, China

*chenyushuang@sinap.ac.cn

Keywords: PRINTED CIRCUIT HEAT EXCHANGER, MOLTEN SALT, INLET HEADER, FLOW DISTRIBUTION, NUMERICAL SIMULATION

Abstract

Printed Circuit Heat Exchanger (PCHE) can be used as the heat transfer device for high-temperature molten salt reactors due to its high efficiency and compact structure. However, PCHE is a typical multi-channel heat exchanger. The flow distribution in the PCHE channels is significantly influenced by geometric design and operating conditions. Flow maldistribution among channels can lead to temperature non-uniformity, which adversely impacts heat transfer performance and overall system efficiency. In this study, numerical simulation is used to investigate the effect of inlet header structure on flow distribution in the straight-channel PCHE. A modified inlet header with a flow homogenizer is designed. The influence of geometric parameters on flow maldistribution among channels is systematically analysed, such as header width, inlet pipe diameter, and the arrangement of perforations on the flow homogenizer. The results indicate that the header structure has a significant impact on the uniformity of flow distribution. With modified geometric parameters, the inlet header with flow homogenizer reduced the maximum deviation in flow distribution to 1.7%. The result meets the requirements of engineering design and provides an important reference for the design of molten salt reactors.

1 Introduction

Molten salt reactor (MSR) is one of the six candidate reactor types for the Generation IV advanced nuclear energy systems. Due to the favorable thermal properties of molten salt, such as high specific heat capacity, excellent thermal conductivity, and chemical stability, MSRs offer advantages including high energy density, high-temperature output, and the potential for compact, low-cost modular reactor designs^[1]. The printed circuit heat exchanger (PCHE), characterized by its high temperature and pressure resistance and compact structure, is one of the candidate heat exchangers in high-temperature molten salt reactors. The structure of the PCHE makes it an ideal choice for efficient heat exchange. However, as a typical multi-channel plate-type heat exchanger, PCHE is inherently susceptible to flow maldistribution and temperature non-uniformity. These issues can lead to localized overheating or insufficient cooling, directly affecting the thermal performance. In more severe cases, such non-uniformities may cause the exchanger to deviate from stable operating conditions, thereby significantly reducing its overall thermal efficiency^[2]. Therefore, improving the uniformity of flow distribution among channels is essential for enhancing heat transfer efficiency, ensuring safe and stable operation, and extending the service life of the equipment.

The improvement of fluid distribution in inlet header can be achieved through header shape. Extensive research has been conducted on various header shapes. Ma et al.^[3] established a complete PCHE model to predict the flow distribution. The

results indicated that inlet and outlet local hydraulic losses are the primary causes of the flow maldistribution. To improve the flow distribution, adjustments to channel lengths and flow rates were proposed. Chu et al.^[2] numerically analysed the influence of four different inlet headers on flow distribution and proposed a novel modified hyperbolic inlet header based on the streamline profile. This configuration reduced the flow non-uniformity by 46% compared with the practical manufactured model. Simultaneously, the improvement of flow uniformity by the hyperbolic inlet header increased the overall thermal-hydraulic performance of the PCHE by 39.5%. Manikanda et al.^[4] conducted experimental and numerical studies on the flow maldistribution. The results showed that trapezoidal headers exhibit significantly lower flow non-uniformity compared to rectangular and triangular headers. The suitable width and depth of the header can effectively improve the flow uniformity among channels. Anbumeenakshi et al.^[5] investigated the effects of different header shapes and inlet configurations on flow maldistribution in microchannel heat exchangers. Experimental analyses were conducted on rectangular, trapezoidal, and triangular headers under varying flow rates. The results indicated that the flow distribution was simultaneously influenced by the shape of the header, inlet configuration, and flow rate. Habib et al.^[6] conducted numerical investigations on the flow field at the entrance of the heat exchanger. The study analysed the effects of flow velocity, inlet pipe diameter, pipe position, geometric configuration, and the secondary header on flow maldistribution. Wang et al.^[7] numerically analysed that vortex formation occurred as the flow passed through the

inlet header, which increased flow maldistribution. The study showed that introducing a transition section could significantly reduce vortex regions. Furthermore, an improved hyperbolic inlet header structure was proposed, and the optimized design reduced flow non-uniformity by 50% and 21%, respectively, depending on the header shape. Yang et al.^[8] proposed a quasi-S header configuration that reduces the geometric mutation as well as extends the hydraulic path between the exchanger core and inlet duct. Numerical results indicated that this design improves flow uniformity while mitigating heat transfer deterioration and pressure drop. Feng et al.^[9] proposed a modified manifold with bent fins and airfoil fins to improve the flow non-uniformity and temperature distribution. Numerical results showed that, compared to the free manifold and straight rib manifold, the flow non-uniformity of the modified manifold was reduced by 39.4% and 61.8%, respectively. Furthermore, the overall performance was increased by 5% and 8.5%, respectively.

Additionally, multiple methods can be employed to enhance flow distribution in headers. Peng et al.^[10] proposed an inlet header configuration with splitter plates, and determined geometric parameters such as the number of splitter plates, the inclined angle of outermost plates, and the height of splitter plates. Numerical results showed that the optimized header configuration reduced flow maldistribution and pressure drop by 91.5% and 40.9%, respectively. Men et al.^[11] proposed a drop-shaped baffle to improve fluid distribution and surface temperature distribution by adjusting the header shape parameters and the baffle parameters. Compared with conventional heat sinks, the maximum temperature was reduced by 12.12%–14.62%, the pressure drop decreased by 2.78%–4.44%, and the standard deviation of volumetric flow rate was reduced by 68.32%. Wen et al.^[12] investigated the flow characteristics at the entrance of a plate-fin heat exchanger using particle image velocimetry (PIV) and numerical simulations. The results indicated that the introduction of a punched baffle, the number of vortices was significantly reduced, and the flow distribution uniformity was improved in both axial and radial directions. Kim et al.^[13] studied the flow uniformity among channels through numerical simulations. To enhance flow uniformity, a perforated plate was installed in the inlet header, with local hole diameters determined based on the local flow velocities when the plate was not installed. The results showed a significant improvement in flow uniformity. Furthermore, the accuracy of the numerical simulation was validated using PIV. Wei et al.^[14] validated the effectiveness of baffle insertion for achieving target flow distributions through numerical simulations and PIV technique. The robustness study implied that for uniform fluid flow distribution, the optimal baffle could be used within a relatively wide range of inlet flow rates. Wang et al.^[15] conducted experimental comparisons among rectangular, trapezoidal, multi-step, baffle plate and baffle tube headers. The results demonstrated that the flow distribution was highly dependent on the header shape and the total flow rate. The use of baffle tubes effectively suppressed vortex formation and significantly improved the uniformity of flow distribution. Chu et al.^[16] analysed the effects of four modified inlet manifolds on flow

maldistribution, including inclined baffle, segmental baffle, helical baffle, and improved helical baffle. Numerical simulation results showed that all baffle configurations contributed to improving flow uniformity among channels. The inlet manifold with improved helical baffle achieved the best performance, reducing flow non-uniformity by 52% and increasing the Nusselt number by 24%. Qin et al.^[17] designed an inlet header with a hot helium flow homogenizer. The non-uniformly arranged square holes on the homogenizer increased flow resistance and reduced pressure difference, thereby effectively improving the inter-unit flow rate uniformity. Compared with the current inlet structure with a baffle, the maximum inter-unit flow rate deviation was decreased from 2.97% to 0.30%.

As seen from references mentioned above, flow maldistribution is a common issue in multi-channel heat exchangers. The factors leading to this problem include the header structure, channel length, fluid properties and velocities, and the position of the inlet pipe. Among these, the header structure is considered as the primary factor affecting flow uniformity among channels. Previous studies have primarily investigated header optimization using working fluids such as water, supercritical carbon dioxide, and helium through experimental and numerical methods.

In this study, molten salt is used as the working fluid, and the flow characteristics in the inlet header is analysed numerically. An inlet header with a flow homogenizer is proposed to enhance flow uniformity. Three different header structures are compared in terms of their flow distribution. The influence of geometric parameters on the flow maldistribution among channels is systematically analysed, including header width, inlet pipe diameter, and the arrangement of perforations on the flow homogenizer.

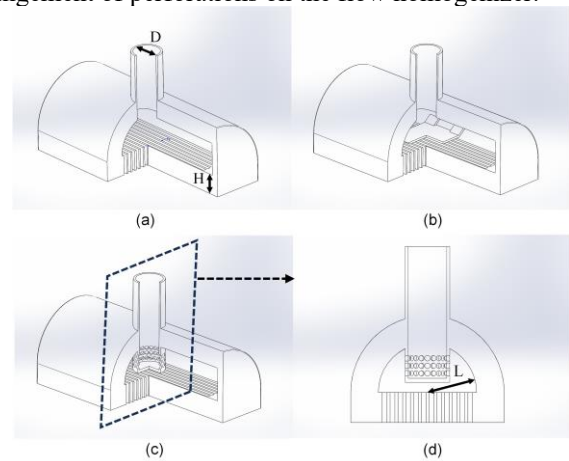


Fig. 1 Schematic diagram of inlet headers. (a) baseline design, (b) inlet header with baffle, (c) inlet header with flow homogenizer, (d) Header cross-section with flow homogenizer

2. Methodology

2.1. Geometric model

The PCHE typically consists of inlet and outlet headers and a heat exchanger core containing numerous microchannels.

Modeling the entire microchannels would significantly increase computational cost. To reduce mesh count and improve computational efficiency, the geometry is simplified in this study. The developed model includes only the entrance of heat exchanger, including the inlet pipe, the inlet header, and 12 shortened core channels.

A semi-cylindrical inlet header configuration is adopted, and three different inlet headers are investigated, as shown in Fig. 1. Fig. 1(a) shows the baseline header; Fig. 1(b) presents an inlet header with a baffle; Fig. 1(c) and (d) show an inlet header with a flow homogenizer. The diameter of the inlet pipe D is 77 mm, the header width L is 98 mm, and the channel length H is 60 mm. The flow homogenizer is a cylindrical extension of the inlet pipe, with three rows of perforations (20 holes per row) uniformly distributed on the cylindrical wall. The diameter of each perforation is 11 mm, and the inner diameter of the flow homogenizer matches that of the inlet pipe (77 mm). Except for the presence of the baffle and flow homogenizer, all other geometric parameters of the inlet headers are identical.

2.2 Physical model

The fluid flow in this study is assumed to be steady-state with no internal heat source. The molten salt is assumed to have a uniform temperature at the inlet. The RNG κ - ϵ turbulence model with the enhanced wall functions is used for the simulation. Shi et al.^[18] validated that the RNG κ - ϵ model with enhanced wall functions can accurately predict the flow and heat transfer characteristics of molten salt in a PCHE. The maximum deviation between the simulation and experimental results was within $\pm 12\%$. The governing equations adopted in the study include continuity equation, momentum equation, energy equation, and RNG κ - ϵ equations with enhanced wall functions. The steady-state equations are shown in Eqs. (1) – (5).

Continuity equation:

$$\frac{\partial}{\partial x_i}(\rho u_i) = 0 \quad (1)$$

Momentum equation:

$$\frac{\partial}{\partial x_i}(\rho u_i u_j) = -\frac{\partial p}{\partial x_i} + \frac{\partial}{\partial x_j} \left[(\mu + \mu_t) \left(\frac{\partial u_i}{\partial x_j} + \frac{\partial u_j}{\partial x_i} - \frac{2}{3} \frac{\partial u_i}{\partial x_i} \delta_{ij} \right) \right] + \rho g_i \quad (2)$$

Energy equation:

$$\frac{\partial}{\partial x_i}(\rho u_i h) = \frac{\partial}{\partial x_i} \left[C_p \left(\left(\frac{\mu}{Pr} + \frac{\mu_t}{Pr_t} \right) \frac{\partial T}{\partial x_i} \right) \right] \quad (3)$$

κ equation:

$$\frac{\partial}{\partial x_i}(\rho k u_i) = \frac{\partial}{\partial x_i} \left(\alpha_k \mu_{eff} \frac{\partial k}{\partial x_i} \right) + G_k + G_b - \rho \epsilon \quad (4)$$

ϵ equation:

$$\frac{\partial}{\partial x_i}(\rho \epsilon u_i) = \frac{\partial}{\partial x_i} \left(\alpha_\epsilon \mu_{eff} \frac{\partial \epsilon}{\partial x_i} \right) + C_{1\epsilon} \frac{\epsilon}{k} (G_k + C_{3\epsilon} G_b) - C_{2\epsilon} \rho \frac{\epsilon^2}{k} - R_\epsilon \quad (5)$$

Table 1 Material parameters

Parameters	FNaBe
Density / $\text{g}\cdot\text{cm}^{-3}$	$\rho = 2.27 - 0.37 \times 10^{-3} T$
Specific heat capacity / $\text{J}\cdot(\text{kg}\cdot\text{K})^{-1}$	2177
Dynamic viscosity / $\text{Pa}\cdot\text{s}$	$\eta = 3.453 \times 10^{-7} T^2 - 0.000696T + 0.357$
Thermal conductivity / $\text{W}\cdot(\text{m}\cdot\text{K})^{-1}$	0.87

The boundary conditions for the flow field are set as follows:

- (1) Inlet boundary: The molten salt has a mass flow rate of $0.710 \text{ kg}\cdot\text{s}^{-1}$ and a temperature of 903 K;
- (2) Outlet boundary: Pressure outlet boundary;
- (3) Wall boundary: Adiabatic no-slip walls.

The entire governing equations are solved by FLUENT software with double precision. The COUPLED algorithm was employed to solve the pressure–velocity coupling equations. A second-order upwind scheme was used for the convection terms, and the convergence criterion for all residuals was set to 10^{-6} .

The molten salt used in the study is FNaBe, whose thermophysical properties change with temperature, as listed in Table 1.

2.3 Data Reduction

To evaluate the flow distribution performance of the PCHE inlet header, the maximum deviation and non-uniformity are adopted as the evaluation criteria for flow maldistribution. The maximum deviation is defined as:

$$d = \frac{Q_{\max} - Q_{\min}}{Q_{\text{avg}}} \quad (6)$$

The non-uniformity S represents the dispersion degree of flow distribution among channels. A smaller value of S indicates a more uniform flow distribution. The non-uniformity S is calculated as:

$$S = \sqrt{\frac{1}{N-1} \sum_{i=1}^N \left(\frac{Q_i - Q_{\text{avg}}}{Q_{\text{avg}}} \right)^2} \quad (7)$$

where N is the number of channels, i is the outlet index, Q_i denotes the mass flow rate in the i -th channel, and Q_{ave} is the average mass flow rate among all channels.

2.4 Mesh independence analysis

The baseline design is selected to verify grid independence. The mesh is generated using Fluent Meshing and Poly-Hexcore meshes was employed. The effect of different mesh number on the simulation results is shown in Fig. 2. The non-uniformity differs by less than 1% between the cases with 11.51 million and 20.14 million cells. Therefore, to ensure computational efficiency while maintaining simulation accuracy, the mesh with 11.51 million cells is adopted for subsequent simulations.

3 Results

3.1 Effect of inlet headers

Fig. 3. illustrates the velocity contour of the baseline inlet header. After the fluid enters the header from the inlet pipe, a sudden geometric expansion leads to the formation of strong velocity gradients and vortices. The velocity in the central region is significantly higher than that in the peripheral areas, causing the central channels to receive a larger share of the flow. Although higher flow rates can enhance heat transfer, they also result in increased pressure loss. As a result, flow maldistribution significantly undermines the overall thermal performance of the PCHE. In addition, the non-uniform flow distribution leads to uneven temperature fields, which may induce thermal stresses, potentially compromising the operational stability and safety of the heat exchanger. Therefore, it is essential to optimize the geometric design of the heat exchanger. Incorporating flow-guiding structures into the inlet header is one of the common methods to improve flow uniformity. The baseline header is shown in Fig. 1(a). Fig. 1(b) shows an inlet header with a baffle, a typical guiding structure used to improve flow uniformity. In this study, a modified inlet header with a flow homogenizer is proposed, as shown in Fig. 1(c).

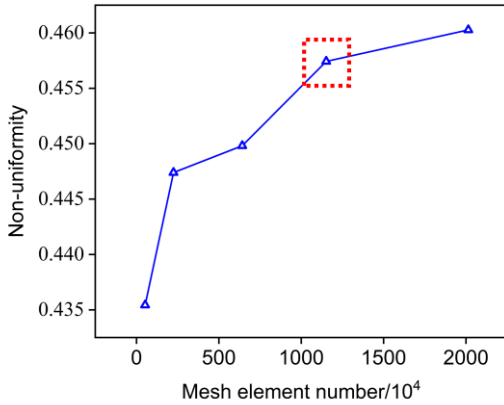


Fig. 2 Grid independence analysis

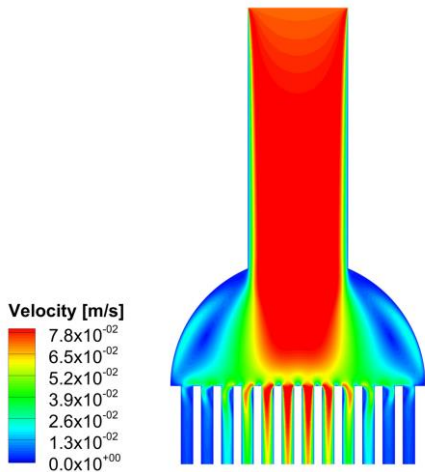


Fig. 3 Velocity Contour in baseline design

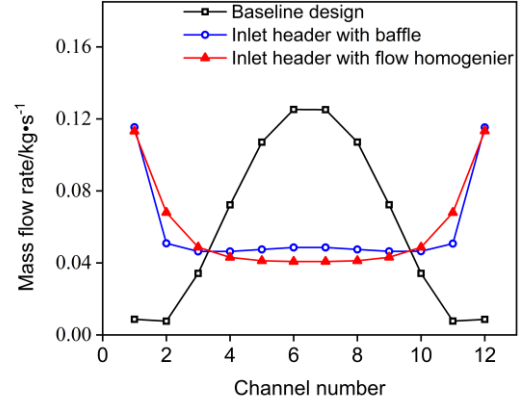


Fig. 4 Mass flow rates in channels of inlet headers

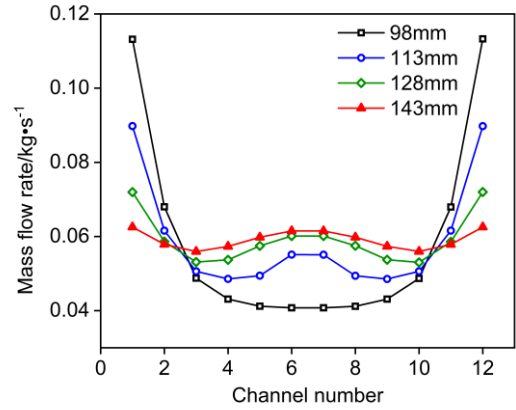


Fig. 5 Mass flow rates in channels with different widths

The mass flow rate distributions among channels for the baseline header, inlet header with baffle, and inlet header with a flow homogenizer are compared in Fig. 4. For the baseline header, the mass flow rates in the central channels (channels 6 and 7) are more than ten times higher than those in the peripheral channels (channels 1 and 12). With the introduction of a baffle, the excessive flow through the central channels is partially suppressed, and the direct high-velocity impact of molten salt on the central heat exchange structure is reduced. This results in a smoother overall flow distribution; however, noticeable maldistribution still remains. When the flow homogenizer is adopted, the flow becomes more evenly distributed among all channels, and the difference between central and peripheral flow rates is significantly reduced. The non-uniformity and maximum deviation are 0.46 and 122.56% for the header with the perforated homogenizer. Subsequent sections analyse the influence of header width, inlet pipe diameter, and perforation on the flow distribution, aiming to improve flow uniformity through local geometric optimization.

3.2 Effect of header length on flow maldistribution

Fig.5 compares the mass flow rate distribution among channels for inlet headers with different widths. When the header width is 98 mm, the mass flow rates in the peripheral channels (Channels 1 and 2) are significantly higher than

those in the central channels, resulting in a non-uniformity of 0.46 and a maximum deviation of 122.56%. As the header width increases, the difference in mass flow rate between channels gradually decreases. The flow rates in the central channels increase, while those in the peripheral channels decline significantly. When the header width reaches 143 mm, the non-uniformity decreases to 0.041 and the maximum deviation to 11.13%. Although flow uniformity improves with increasing header width, the physical size of the heat exchanger in practical applications imposes constraints.

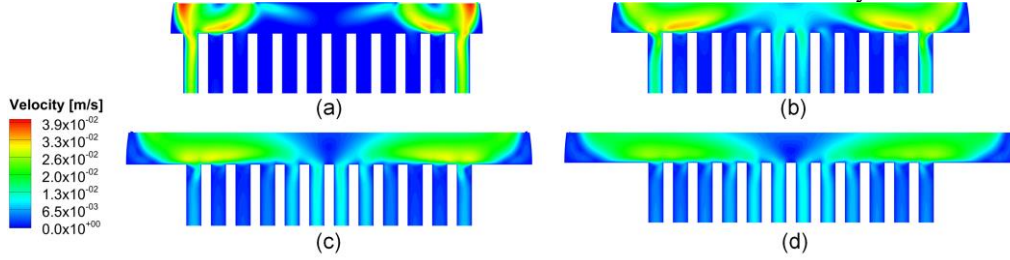


Fig. 6 Velocity contours with different widths (a)98mm, (b)113mm, (c)128mm, (d)143mm

3.3 Effect of inlet pipe diameter on flow maldistribution

Fig. 7 presents the influence of inlet pipe diameter on the non-uniformity and maximum deviation among channels under a header width of 143 mm. Five different inlet pipe diameters (77 mm, 81 mm, 85 mm, 89 mm and 93 mm) are compared. The results indicate that smaller diameters lead to poorer flow uniformity. When the diameter is 77 mm, the non-uniformity and maximum deviation are 0.041 and 11.13%, respectively. When the diameter is increased to 93 mm, these values decrease to 0.029 and 7.49%, respectively. This trend suggests that, within a certain range, increasing the inlet pipe diameter promotes more uniform flow distribution among channels.

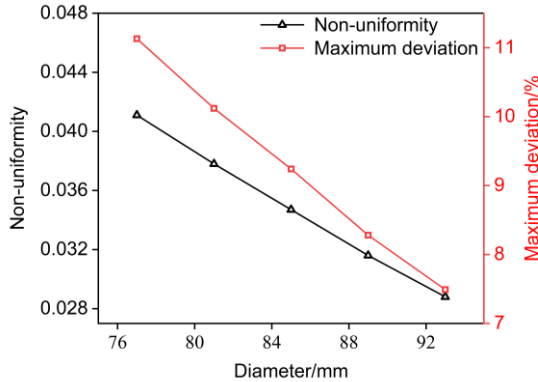


Fig. 7 Effect of inlet pipe diameter on non-uniformity and maximum deviation

Fig. 8 displays the velocity contours in the inlet header for inlet pipe diameters of 77 mm (Fig. 8a) and 93 mm (Fig. 8b). As the inlet diameter increases, the cross-sectional area also increases. Given a constant inlet mass flow rate, the average velocity in the inlet pipe decreases accordingly. The reduced velocity facilitates better flow development and redistribution. According to the results of non-uniformity and maximum deviation, lower flow velocities promote more uniform distribution of fluid among the channels. A larger inlet

Therefore, a trade-off between structural size and performance must be considered in actual design.

Fig. 6 shows the velocity contours in the inlet header with different header widths. As the header width increases, the internal flow area becomes larger, allowing the fluid more space to diffuse laterally and to develop a velocity component directed toward the central region. Consequently, the flow shifts inward, and the mass flow rate in the peripheral channels is significantly reduced. In addition, regions of high velocity gradient and vortex formation are reduced, leading to a more uniform overall velocity distribution.

diameter not only lowers local flow velocity but also suppresses vortex formation, thereby improving the velocity distribution in the header.

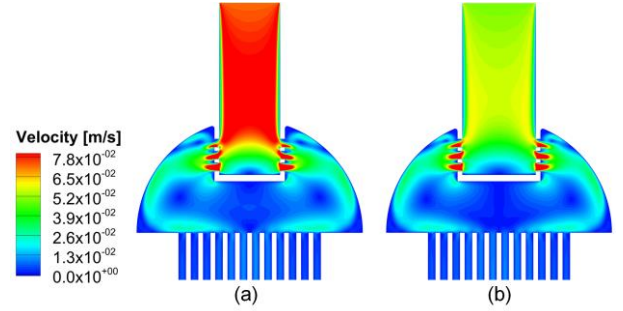


Fig. 8 Velocity contours with different pipe diameters (a)77mm, (b)93mm

3.4 Effect of perforation arrangement on flow maldistribution

To reduce the deviation in mass flow rates among channels, six different flow homogenizer configurations were designed, with their design parameters summarized in Table 2. Under the condition that the total flow area of the perforations on the cylindrical wall remains constant, the variations among designs primarily involve the number of perforation rows, the number of perforations per row, and the diameter of the perforations. Flow homogenizers No. 1 to No. 5 differ in the perforation arrangement on the cylindrical wall, while homogenizer No. 6 is based on No. 4 with additional perforations introduced on the end wall.

Table 3 presents the mass flow rates among the 12 channels of the inlet header with six different flow homogenizers, along with the corresponding maximum deviation (d) and non-uniformity (S). The results indicate that increasing the number of perforations can effectively reduce flow non-uniformity. No. 4 achieves a maximum deviation of 4.52%. However, further increasing the perforation number, as in homogenizer No. 5, yields limited improvement and may lead to excessively small spacing between holes. To address

the issue of higher flow rates in the peripheral channels compared to the central ones, homogenizer No. 6 introduces additional perforations on the end wall to redirect part of the flow toward the central channels. Figure 9 shows the velocity contours for homogenizers No. 1, 4, and 6, which clearly demonstrate this trend. An increased number of perforations on the cylindrical wall guides more fluid toward the central region, and once the improvement from the perforations on the cylindrical wall reaches a saturation point, the end-wall perforations further enhance the flow distribution. As a result, homogenizer No. 6 reduces the maximum deviation to as low as 1.7%.

Table 2 Design parameters of flow homogenizers

Case No.	perforations arrangement on the cylindrical wall		Diameter of perforations on the end wall /mm
	Row	perforations /row	
1	3	20	--
2	5	20	--

3	5	30	--
4	6	30	--
5	8	40	--
6	6	30	3.6

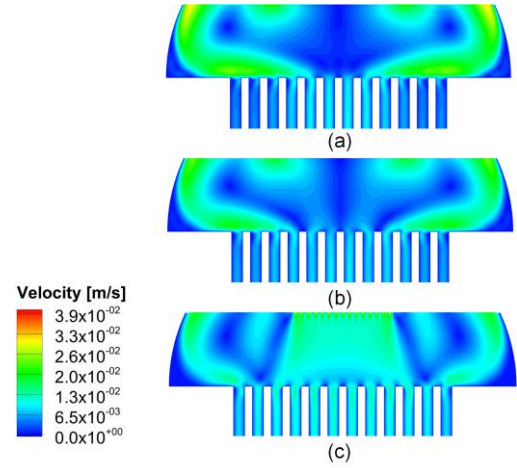


Fig. 9 Velocity contours of different perforation arrangement

Table 3 Effect of perforation arrangement on flow maldistribution

Case No.	Mass flow rates of each channel (10^{-3}kg/s)												d (%) S	
	1	2	3	4	5	6	7	8	9	10	11	12		
1	61.3	57.8	56.8	58.3	62	60.9	60.9	60	58.3	56.8	57.8	61.3	7.5	0.041
2	61.2	58.7	57.8	58.6	59.2	59.5	59.5	59.2	58.6	57.8	58.7	61.2	5.8	0.019
3	61.0	58.9	58.2	58.7	58.9	59.3	59.3	58.9	58.7	58.1	59	61.1	4.9	0.016
4	60.9	59.0	58.2	58.7	58.8	59.3	59.3	58.8	58.7	58.2	59	60.9	4.5	0.014
5	61	59.3	58.5	58.7	58.5	59.0	59.0	58.5	58.7	58.5	59.3	61	4.3	0.015
6	58.7	59.7	59.4	59.0	58.8	59.4	59.4	58.8	59.0	59.3	59.7	58.7	1.7	0.006

4 Conclusion

The effect of inlet headers on flow maldistribution of molten salt in straight-channel PCHE was numerically investigated. A modified inlet header with a flow homogenizer was proposed to significantly improve flow distribution among channels. The investigation focused on the effects of header width, inlet pipe diameter, and the perforation arrangement of the flow homogenizer on the mass flow rates among channels. The major conclusions are as follows:

1. The inlet header with flow homogenizer effectively mitigates the high-velocity impact of molten salt on the central heat exchange channels, thereby reducing the mass flow rate in the central channel and significantly enhancing the overall flow uniformity.
2. For inlet headers with a flow homogenizer, the header length is a critical geometric parameter influencing flow uniformity. Increasing the header length facilitates lateral diffusion of fluid in the header and reduces the regions of high velocity gradients and vortex formation caused by abrupt structural changes. As the header length increases

from 98 mm to 143 mm, the maximum flow rate deviation decreases from 122.56% to 11.13%.

3. Enlarging the inlet pipe diameter lowers the flow velocity entering the flow homogenizer. lower velocity promotes better flow development and redistribution while also suppressing vortex formation, leading to improved flow uniformity among channels.
4. By optimizing the perforation arrangement on the cylindrical and end walls of the flow homogenizer, the modified inlet header effectively improves the flow distribution. The maximum deviation is reduced to 1.7%, making it a promising header design for enhancing the heat transfer performance of the PCHE.

5 Acknowledgements

This work is supported by the “Gansu Major Scientific and Technological Special Project under Grant (Grant No. 23ZDGH001) and “Youth Innovation Promotion association, Chinese Academy of Science” (Grant No. 2020263).

6 References

- [1] H. -J. Xu, Z. -M. Dai, X. -Z. Cai, et al. Thorium Molten Salt Reactor and Comprehensive Utilization of Nuclear Energy [J]. 2018, Modern Physics Knowledge, 30(04), 25-34. (in Chinese)
- [2] W.-x. Chu, K. Bennett, J. Cheng, et al. Numerical study on a novel hyperbolic inlet header in straight-channel printed circuit heat exchanger [J]. 2019, Applied Thermal Engineering, 146, 805-814.
- [3] T. Ma, P. Zhang, H. Shi, et al. Prediction of flow maldistribution in printed circuit heat exchanger [J]. 2020, International Journal of Heat and Mass Transfer, 152, 119560.
- [4] R. Manikanda Kumaran, G. Kumaraguruparan, T. Sornakumar. Experimental and numerical studies of header design and inlet/outlet configurations on flow mal-distribution in parallel micro-channels [J]. 2013, Applied Thermal Engineering, 58(1), 205-216.
- [5] C. Anbumeenakshi, M. R. Thansekhar. Experimental investigation of header shape and inlet configuration on flow maldistribution in microchannel [J]. 2016, Experimental Thermal and Fluid Science, 75, 156-161.
- [6] M. A. Habib, R. Ben-Mansour, S. A. M. Said, et al. Evaluation of flow maldistribution in air-cooled heat exchangers [J]. 2009, Computers & Fluids, 38(3), 677-690.
- [7] Y. Wang, Y. Lu, Y. Wang, et al. Structural Optimization of the Inlet Header of Supercritical Carbon Dioxide Printed Circuit Board Heat Exchanger [J]. 2024, Journal of Thermal Science, 33(4), 1458-1467.
- [8] H. Yang, J. Wen, X. Gu, et al. A mathematical model for flow maldistribution study in a parallel plate-fin heat exchanger [J]. 2017, Applied Thermal Engineering, 121, 462-472.
- [9] F. Jin, D. Chen, L. Hu, et al. Numerical study on flow distribution of supercritical CO₂ in multiple channels of printed circuit heat exchanger [J]. 2023, Applied Thermal Engineering, 234, 121185.
- [10] X. Peng, D. Li, J. Li, et al. Improvement of Flow Distribution by New Inlet Header Configuration with Splitter Plates for Plate-Fin Heat Exchanger [J]. 2020, Energies, 13(6), 1323.
- [11] Z. Men, Q. Hu, W. Chen. Parametric model and experimental investigation of a distribution header to relieve heat sink coolant maldistribution [J]. 2024, International Communications in Heat and Mass Transfer, 159, 108149.
- [12] J. Wen, Y. Li, A. Zhou, et al. An experimental and numerical investigation of flow patterns in the entrance of plate-fin heat exchanger [J]. 2006, International Journal of Heat and Mass Transfer, 49(9), 1667-1678.
- [13] M.-H. Kim, V. T. Nguyen, S. Im, et al. Experimental Validation of Flow Uniformity Improvement by a Perforated Plate in the Heat Exchanger of SFR Steam Generator [J]. 2021, Energies, 14(18), 5846.
- [14] M. Wei, G. Boutin, Y. Fan, et al. Numerical and experimental investigation on the realization of target flow distribution among parallel mini-channels [J]. 2016, Chemical Engineering Research and Design, 113, 74-84.
- [15] C.-C. Wang, K.-S. Yang, J.-S. Tsai, et al. Characteristics of flow distribution in compact parallel flow heat exchangers, part II: Modified inlet header [J]. 2011, Applied Thermal Engineering, 31(16), 3235-3242.
- [16] W.-x. Chu, T. Ma, M. Zeng, et al. Improvements on maldistribution of a high temperature multi-channel compact heat exchanger by different inlet baffles [J]. 2014, Energy, 75, 104-115.
- [17] H. Qin, X. Luo, X. Li, et al. Numerical Investigation of Hot Helium Flow Homogenizer on Inter-Unit Flow Rate Uniformity of HTGR Once Through Steam Generator [J]. 2022, Frontiers in Energy Research, Volume 10 - 2022.
- [18] H.-Y. Shi, M.-J. Li, W.-Q. Wang, et al. Heat transfer and friction of molten salt and supercritical CO₂ flowing in an airfoil channel of a printed circuit heat exchanger [J]. 2020, International Journal of Heat and Mass Transfer, 150, 119006.